In-depth Analysis of Unsupervised Clustering for Female Breast Shape

Haoyang Xie, Xi Chen, Zhicai Yu, Yueqi Zhong, and Kai Lu

***Abstract*—Female breast shape is significantly essential for female healthcare, bra design, etc. However, there is no authoritative standard for breast shape classification. In this paper, we analysis the female breast category by unsupervised clustering the horizontal female breast contours. Specifically, the Elliptic Fourier Descriptors (EFDs), extracted from breast contour, are employed as the contour features. Subsequently, we use PCA to reduce the feature into lower dimensions. Experiments demonstrate that the lower dimensions are enough to present the original features. Then, we employ two widely used clustering algorithms, K-Means++ and FCM, to cluster the female breast contours, and deeply analyze and compare the results of two clustering results in terms of effectiveness. Experimental results demonstrate that the K-Means++ is more suitable for female breast contour clustering, and the results are more reasonable than FCM.**

***Index Terms*—Elliptic Fourier Analysis, elliptic fourier descriptor, female breast clustering, clustering validation, PCA.**

I. Introduction

Female brassiere plays a vital role in female daily life, which supports female breasts to provide concealment and to prevent the breasts from sagging [1]. However, the complexity in breast shape and variations in shape and size make it difficult to design a fit brassiere. According to studies, about 70% of females are wearing incorrectly sized brassieres [2]-[4]. Thus, it is worth to research and analyze the shape of the female breasts, which will contribute to the development of improved sizing systems of brassiere products that work for consumers and manufacturers. For the female breast shape, the horizontal contour is the most important parameter [5], which contains lots of valuable information such as width, depth, girth, etc. Thus, in this paper, we try to classify the female breast shape according to breast contour. Unlike other studies with the ground-truth dataset, there is no authoritative standard for breast shape, i.e., no ground-truth, and we cannot train a supervised network to categorize the shape according to some features or images. All the actual work that focuses on the classification of the female breast is based on unsupervised clustering. However, most of the work does not explain why a particular classification is reasonable. Instead, we deeply compare and analyze the results of two widely used clustering algorithms on female breast classification using mathematical tools.

Early work on female breast sizing classification employs the girth of the breast, under-breast to identify the bra size, and introduce A, B, C, and D to the breast sizing system [6]. With the development of computer hardware and 3D sensor, more research relies on 3D scanning. Zheng *et al*. [5] cluster the female breast shape into eight clusters based on 3D body scans. They use under-breast girth and the breast depth-width ratio as the parametric features. Morris *et al*. [7] study 50 female body shapes and develop a range of 18 various breast shapes. However, the number of clustering is too large to be applied in practice. Dong and Zhang [8] use K-Means to divide the female breast into four categories according to the size of the bar, whereas the method they use to decide the number of clusters is not robust, and they do not study the correctness of this classification. Wang *et al.* [9] subjectively divide the female breast shape into five categories according to anthropometric measurement and do not explain the reasons for such classification.

Generally, much work proposes an approach to classify the female breast but without an in-depth analysis of the results. The main concern of clustering is to reveal the organization of patterns into “sensible” groups, which allows us to uncover the similarities and differences [10]. The results of unsupervised clustering may be different depending on the proprieties of data and input parameters. Evaluating and assessing the results of the clustering methods is referred to as clustering validation [11]. In this paper, we employ two widely used unsupervised clustering algorithms to cluster the female breast shape according to the breast contour. Subsequently, we carefully analyze and compare the clustering results using mathematical methods. Specifically, we employ the Elliptic Fourier Analysis [12] to extract features (Elliptic Fourier Operators, EFDs) from the breast contours and then utilize K-Means++ and Fuzzy C-Means to cluster the female breast shape according to the extracted EFDs. We also prove that the extracted features can reconstruct the original breast curve very well. Subsequently, the two clustering results are analyzed and compared in depth by Scatter and Density between clusters validity index (*S_Dbw*) [13] and Silhouette Width (*SW*) [14]. Both of these indices can evaluate the clustering quality from inter-cluster and intra-cluster.

II. Method

A. Feature Extraction

Given a horizontal breast contour cutting from a 3D human

Manuscript received October 14, 2020; revised April 7, 2021. This work is supported by the National Natural Science Foundation of China (Grant No. 61572124), and the Fundamental Research Funds for the Central Universities (Grant No. CUSF-DH-D-2017006).

Haoyang Xie and Zhicai Yu are with Donghua University, Shanghai, 201620 China (e-mail: xie_haoyang@qq.com, 1039598561@qq.com).

Xi Chen is with SIAS University, Xinzheng, Henan, 451150 China (e-mail: 56908112@qq.com).

Yueqi Zhong is with the Key Lab of Textile Science and Technology, Ministry of Education, and Donghua University, Shanghai (e-mail: zhyq@dhu.edu.cn).

Kai Lu is with Xuchang University, Xuchang, Henan, 461000, China (e-mail: lukai0373@foxmail.com).

doi: 10.18178/ijmlc.2022.12.1.1076

mesh, we extract the Elliptic Fourier Descriptors (EFDs) using Elliptic Fourier Analysis. The *y*-coordinates of each vertex on this horizontal contour are the same. Thus, the breast contour can be approximated at *X-Z* plane as:

$$x_p = A_0 + \sum_{n=1}^{N} a_n cos\frac{2n\pi t_p}{T} + b_n sin\frac{2n\pi t_p}{T} \quad (1)$$

$$z_p = C_0 + \sum_{n=1}^{N} c_n cos\frac{2n\pi t_p}{T} + d_n sin\frac{2n\pi t_p}{T} \quad (2)$$

where t_p is the length from the starting point to the *p-th* point, and the perimeter of the curve is denoted as *T*. *N* is the number of Fourier harmonics requiring to approximate the contours. a_n, b_n, c_n and d_n are the coefficients of Elliptic Fourier for *n-th* harmonic. A_0 and C_0 are the basis coefficients, corresponding to *0* frequency. The Elliptic Fourier Descriptors (EFDs) then could be denoted as a row vector:

$$EFDs = (A_0, C_0, a_1, b_1, c_1, \dots, a_n, b_n, c_n) \quad (3)$$

B. Principal Component Analysis

Technically, the more the harmonics employed in EFA, the higher the dimensions in EFDs. However, excessive harmonic numbers will contain lots of redundant information and increase the complexity of clustering computation. Thus, we employ PCA to reduce the dimensions by representing the features of a subject with a set of principal components (*PCs*). *PCs* are a linear combination of the original EFDs and are demonstrated the real source of variation between shapes.

For each EFDs, the input of PCA can be formatted as a $M \times 4N$ matrix:

$$E_{EFDs} = \begin{bmatrix} a_{11}b_{11}c_{11}d_{11} & \cdots & a_{1N}b_{1N}c_{1N}d_{1N} \\ \vdots & \ddots & \vdots \\ a_{M1}b_{M1}c_{M1}d_{M1} & \cdots & a_{MN}b_{MN}c_{MN}d_{MN} \end{bmatrix} \quad (4)$$

where *M* is the number of the human model in our dataset. Typically, the PCA involved four steps:

1) Calculating the covariance matrix C_{EFDs} of the input E_{EFDs}.
2) Computing the eigenvalues and eigenvectors of C_{EFDs}.
3) Space spanned by the eigenvectors corresponding to the first *k* largest eigenvalues are denoted as a projection matrix $T_{4N\times k}$.
4) $PCs = EFDs \times T_{4N\times k}$ reduces the dimensions from *4N* to *k*, where $k \le 4N$.

C. Error Metric

A contour can be represented by the above features, and the contour can also be reconstructed using the reduced-dimensional EFDs. To evaluate the reconstruction, we employ three metrics to measure the error between the original breast contour and reconstructed contour: mean distance, standard deviation, and maximum distance between the original and the reconstructed contour.

Taking *O* as the original breast contour and *F* as the reconstructed contour, the mean deviation extent between the original and reconstructed shape,

$$\overline{D} = \frac{1}{N}\sum_{i}^{N} dist(O_i, F_i) \quad (5)$$

where *N* is the total number of the vertices on a contour.

The standard deviation of the distance between the original points and reconstructed points σ_d is the measure of variability, i.e., $\sigma_d = std(D_i)$ .The maximum distance between sampling points and fitting points is denoted as $D_{max} = max\{dist(O_i, F_i)\}, i = 1,2, \dots, K$.

D. Clustering

The final objective of our work is to classify the female breast contours into *K* clusters, which is a typical unsupervised classification problem since the cluster number *K* is unknown. With the extracted *PCs*, we employ two widely used clustering algorithms, K-Means++ and FCM, to classify the breast shape, and analyze the clustering results of these two methods in depth.

K-Means++ cluster can automatically partition the breast contours into *K* groups, which is an improved K-means algorithm proposed by [15]. Compared to the traditional K-Means, the initialization of the *K* centroids is optimized.

In our approach, the number of clusters *K* is estimated by visualizing the error measure W_k, which is an easy-to-use method and demonstrates the inter-cluster dispersion [16]. It is defined as follow,

$$W_k = \sum_{k=1}^{K} \frac{1}{n_r} D_r \quad (6)$$

where $D_r = \sum_{i,i' \in S_r} d_{i,i'}$ is the num of the pairwise distances for all the samples in cluster r. W_r is the inter-cluster sum of the squared distance around the cluster center.

Once *K* is determined, for a given dataset $X \subset R^d, x \in X$, the K-Means++ clustering can be performed according to the following steps:

1) Selecting a cluster center S_l from the input dataset randomly;
2) For each sample *x*, calculating the squared Euclidian Distance $D(x)$ to its near cluster center;
3) Selecting a new cluster center S_i, which maximize the probability $\frac{D(x')}{\sum D(x)}$, where $S_i = x' \in X$;
4) Repeating 2) and 3) until the number of clusters equals *K*;
5) Using the traditional K-Means clustering to minimize the objective function $J_k = \sum_k^K \sum_i^N \parallel x_i - c_k \parallel^2$, where c_k is the *k-th* cluster center, *N* is the number of samples in each cluster, and *K* is the number of clusters.

According to [17], K-Means++ will preserve the structure and distribution of the original data. As an effect to screen the suitable clustering methods for shape categorization, FCM is used to divide the same dataset in the same number of clusters *K*. In order to ensure the robustness of the clustering, the initial centroids are selected randomly rather than using the same initial centroids in K-Means++. The goal of FCM is to minimize the following objective function J_m,

$$J_m = \sum_{i=1}^{N} \sum_{k=1}^{C} u_{ik}^m \parallel x_i - c_k \parallel^2 \\ s.t.\ \sum_{k=1}^{C} u_{ik} = 1, i = 1,2, \dots, N \quad (7)$$

where *m* is the fuzzifier that determines the level of clustering fuzziness. u_{ik} is the degree of membership of x_i in the cluster k. c_k is the *k-th* cluster centroid. *C* is the number of clusters with *C*=*K*. The step-by-step FCM follows.

1) Initializing $U = [u_{ik}]$ matrix, $U^{(0)}$;

2) At j-step, calculating the centroid vectors $C^{(j)} = [c_k]$ with $U^{(j)}$;
3) Updating $U^{(j)}$ and $U^{(j+1)}$ according to the following formula:

$$u_{ik} = \left(\sum_{j=1}^{C} \left(\frac{\|x_i - c_k\|}{\|x_i - c_j\|} \right)^{\frac{2}{m-1}} \right)^{-1} \tag{8}$$

4) Repeating 2) and 3) until $\| U^{(j)} - U^{(j+1)} \| < \epsilon$, where $\epsilon = 0.0001$ is the threshold in our experiments.

E. *Cluster Validation*

The reason we chose two different unsupervised cluster methods is that various clustering algorithms may result in different but similar partitions due to the configuration of parameters. Mathematically, it is possible that these two clustering results are invalid even if both of them look good. There are two reasons for this. The first one is that both results may be improper due to unanticipated occasions caused by parameter configurations. Another one is that the error measure function W_k only evaluate inter-cluster dispersion. Recent studies demonstrates that *S_Dbw* is more effective than other clustering validity indices[13], [14], [18].

S_Dbw validity index combines inter-cluster and intra-cluster similarity and enabled a reliable evaluation of clustering results [18]. The smaller the *S_Dbw*, the more similar the inter-cluster properties, and meanwhile, the more the distinct intra-cluster properties. *S_Dbw* is calculated as follow,

$$S\_Dbw(c) = Dens(c) + Scat(c) \tag{9}$$

where $Dens(c)$ is the inter-cluster density, and $Scat(c)$ is the intra-cluster variance. $Dens(c)$ is calculated as

$$Dens(c) = \frac{1}{C(C+1)} \sum_{i=1}^{C} \sum_{j=1}^{C} \frac{\rho(m_{ij})}{\max\{\rho(v_i), \rho(v_j)\}} \tag{10}$$

where v_i and v_j are centroids of cluster c_i and c_j, respectively. m_{ij} is the middle point of the line segment defined by v_i and v_j. $\rho(m)$ is the density function and defined as

$$\rho(m) = \sum_{l=1}^{n_{ij}} f(x_l, m) \tag{11}$$

where n_{ij} is the number of samples that belong to centroid v_i and v_j. $f(x, m)$ is defined as a piecewise function:

$$f(x,m) = \begin{cases} 1 & if\ d(x,m) > stdev \\ 0 & otherwise \end{cases} \tag{12}$$

where $d(x, m)$ is the squared Euclidean distance. *stdev* is the average standard deviation of the clusters. $Scat(c)$ is calculated as

$$Scat(c) = \frac{1}{C} \sum_{i=1}^{C} \| \frac{\sigma(v_i)}{\sigma(S)} \| \tag{13}$$

where $\sigma(S)$ is the variance of cluster c_i.

F. *Comparison of Clustering*

In practice, the clustering results of K-Means++ and FCM might be similar. Silhouette Width (*SW*) is used to determine the optimal one for breast clustering. For each sample i, its *SW* is defined as:

$$s(i) = \frac{d_{out}(i) - d_{in}(i)}{\max\{d_{out}(i) - d_{in}(i)\}} \tag{14}$$

where $d_{out}(i)$ is the mean distance of sample i to samples in its nearest neighbor cluster. $d_{in}(i)$ is the mean distance of the *i-th* sample in its cluster. In our experiments, squared Euclidean distance is used as the distance function. The averaged $s(i)$, called the score, reflected the overall quality of clustering. The higher the score, the better the quality of the clustering.

III. Experimental Results and Discussion

A. *Dataset*

We have scanned 100 female volunteers, aged from 18-45, using Microsoft Kinect V2 to obtain the 3D mesh under A-pose, and the breast contour curve is extracted according to an automatic human body measurement algorithm proposed by Zhong *et al.*[19]. Body scanning and curve extraction are out of the scope for this paper, and for more details, please refer to [19] and [20].

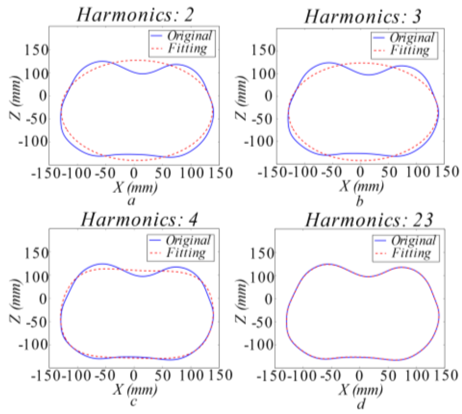

Fig. 1. Reconstruction results of a breast contour with different harmonics.

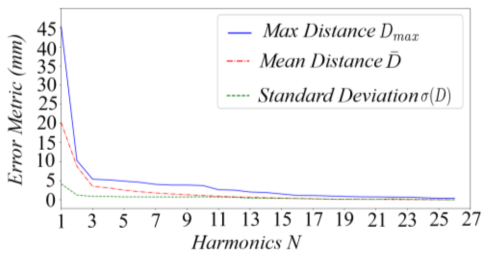

Fig. 2. Relationship between the harmonics and error metric.

B. *Breast Contour Reconstruction*

As we describe above, the features of breast contours can be used to reconstruct the original breast contours, and the reconstruction error can be used to determine the final number of harmonics preserved. For a single contour, different harmonics result in different reconstructions. Fig. 1 demonstrates the changes in reconstruction under various harmonics for a given breast contour. It is clear that as the number of harmonics increase, the reconstruction results are getting better and better. As shown in Fig. 2, the reconstruction errors decrease with the increase of harmonics N. For the breast contours, the maximum distance D_{max}, mean distance $\overline{D}$ and standard deviation σ_D at N=23 are 0.65mm, 0.16mm, and 0.12 mm. From our observation, N=23 is sufficient as replicas for downstream clustering.

C. PCA Results

The EFDs of the entire 100 contours are subject to PCA without any pre-treatment. The first three *PCs* with maximum variance contributions are computed from the EFDs matrix. *PC1*, *PC2* and *PC3* demonstrate 64.21%, 20.12% and 10.35% of the total variation. The total sum (contribution) of them is up to 94.68%, as shown in Fig. 3, which implies that we could use these three components to represent the original features without loss of generality.

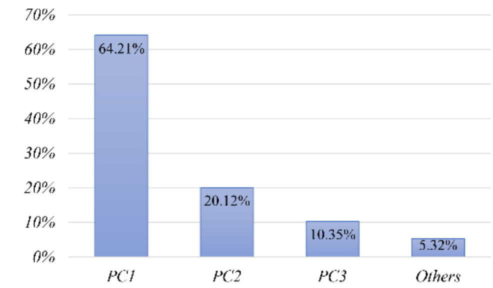

Fig. 3. Contribution of each principal component.

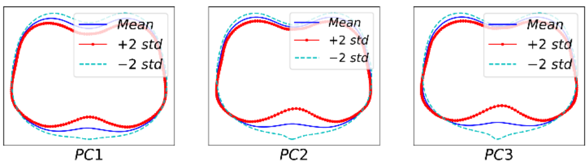

Fig. 4. Influences of PC1, PC2, and PC3 on the breast contour.

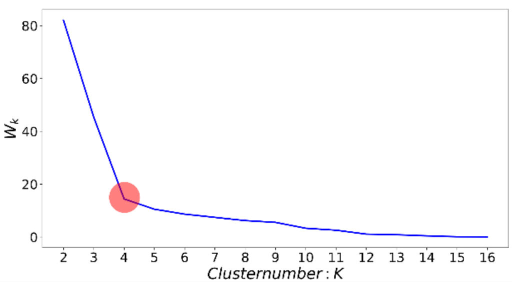

Fig. 5. Relationship between the error metric (W_k) and the number of clusters K.

In order to illustrate the influence of each PC on the breast contour, the mean and ±2 *std* are used to compute a new EFD, which is used to reconstruct three new breast contours. As shown in Fig. 4, *PC*1 demonstrates the flatten degree of the breast contour. *PC*2 and *PC*3 illustrate the curvature variation of the breast curve.

D. Results of Clustering Analysis and Validation

Fig. 5 illustrates the relationship between the error metric W_k and the number of cluster *K*. Obviously, a turning point indicates that the optimal *K* value should be selected as *K=4*. Based on this configuration, we implement K-Means++ and FCM for the entire 100 samples, and Table I and Table II demonstrate the clustering results. The number of samples in each cluster is slightly different since the initialization centroids are selected randomly in our work. Fig. 6 demonstrates the scatter diagram of the results. The ambiguous samples are always located at the boundaries of clusters.

TABLE I: CLUSTERING RESULTS OF K-MEANS++

Cluster	Instance nearest to the centroid	Amount	Description
I	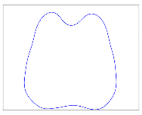	20	A narrower breast but with noticeable breast bulge.
II	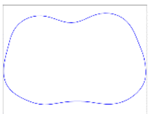	25	A flatter or wider contour without prominent breast bulge.
III	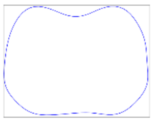	38	A well-rounded breast contour with a natural bulge.
IV	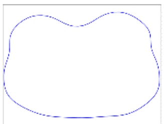	17	A flatter or wider contour with prominent breast bulge because of the concave sections on the left and right sides.

TABLE II: CLUSTERING RESULT OF FCM

Cluster	Instance nearest to the centroid	Amount	Description
I	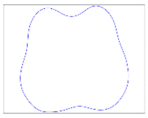	21	A narrower breast but with noticeable breast bulge, similar to K-Means++.
II	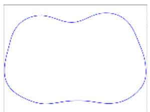	24	A flatter or wider con-tour without noticeable breast bulge, similar to K-Means++.
III	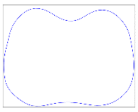	36	A well-rounded breast contour with a natural bulge, similar to K-Means++.
IV	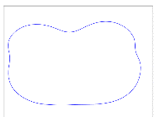	19	A flatter or wider con-tour with prominent breast bulge because of the concave sections on the left and right sides, similar to K-Means++.

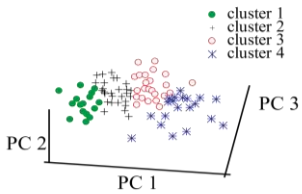

a. K-Means++

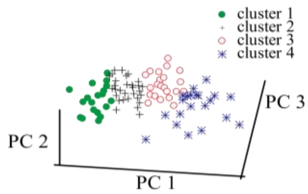

b. FCM

Fig. 6. Clustering results of K-Means++ and FCM.

E. Validation and Comparison of Clustering

As an ambiguous instance, Fig. 7 illustrates a typical phenomenon in clustering. For a given subject, it could be assigned to cluster IV according to K-Means++ but to cluster III according to FCM. Which result is sounder? To answer this question, *S_Dbw* and Silhouette Width (*SW*) are used to validate the clustering properties. Table III lists the results of the validation.

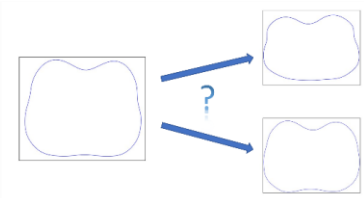

Fig. 7. An ambiguous instance. It is assigned to cluster IV according to K-Means++, but to cluster III based on FCM.

TABLE III: *S_Dbw* FOR K-MEANS++ AND FCM

K	2	3	4	5	6	7	8
K-Means++	0.82	0.62	**0.52**	0.9	0.71	0.93	0.86
FCM	0.82	0.62	**0.52**	0.91	0.71	0.94	0.86

It is shown that both minimum values of *S_Dbw* on these two cluster methods are obtained at *K=4*, which further proves that the cluster number *K=4* is an optimal solution for both K-Means++ and FCM. With this number, the average *SW* of each method is calculated to assess the quality of clustering. Fig. 8 demonstrates that the score of K-Means++ is slightly higher than that of FCM. Hence, K-Means++ is more appropriate for the clustering of female breast shape, and the example demonstrated in Fig. 7 should be classified into clustering IV according to K-Means++.

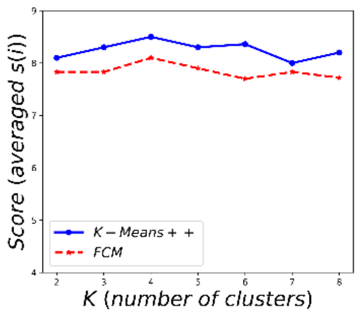

Fig. 8. Comparison of the score (average $s(i)$) between K-Means++ and FCM.

IV. Conclusion

In this paper, we investigate the methods of clustering the horizontal shape of female breasts. Female breast contours are extracted from 3D human mesh using previous algorithms, and we employ EFA to extract the original features of breast contour. Subsequently, in order to reduce the redundant information and the dimensions of features, the EFDs are feed into PCA to obtain a lower feature space. Experiments demonstrate that the first three principal components are enough to demonstrate the 23-D FEDs. Also, we employ two widely used clustering algorithm K-Means++ and FCM to cluster the breast contour. Unlike other works, we deeply analyze and compare the results of two clustering algorithm on female breast contours, and present that K-Means++ is more reasonable for the classification of female breast contours. Finally, the female breast can be clustered into four categories, and our work could contribute to the development of improved sizing systems of brassiere products that work for consumers and manufacturers.

Conflict of Interest

The authors declare no conflict of interest.

Author Contributions

Haoyang Xie conducted the research; Xi Chen collected and analyze the data; Zhicai Yu and Kai Lu set up the experimental environment; Haoyang Xie and Yueqi Zhong wrote the paper; All authors had approved the final version.

References

[1] J. Farrell-Beck, L. Poresky, J. Paff, and C. Moon, "Brassieres and women's health from 1863 to 1940," *Cloth. Text. Res. J.*, vol. 16, no. 3, pp. 105-115, 1998.

[2] A. Greenbaum, T. Heslop, J. Morris, and K. Dunn, "An investigation of the suitability of bra fit in women referred for reduction mammaplasty," *Br. J. Plast. Surg.*, vol. 56, no. 3, pp. 230-236, 2003.

[3] K. Wood, M. Cameron, and K. Fitzgerald, "Breast size, bra fit and thoracic pain in young women: a correlational study," *Chiropr. Osteopat.*, vol. 16, no. 1, pp. 1, 2008.

[4] D. E. McGhee and J. R. Steele, "Optimising breast support in female patients through correct bra fit. A cross-sectional study," *J. Sci. Med. Sport*, vol. 13, no. 6, pp. 568-572, 2010.

[5] R. Zheng, W. Yu, and J. Fan, "Development of a new Chinese bra sizing system based on breast anthropometric measurements," *Int. J. Ind. Ergon.*, vol. 37, no. 8, pp. 697-705, 2007.

[6] K. Bressler, K. Newman, and G. Proctor, *A Century of Style: Lingerie*. Quarto Publishing Plc., London, 1998.

[7] D. Morris, J. Mee, and H. Salt, "The calibration of female breast size by modeling," in *Proc. International Foundation of Fashion Technology Institutes Conference, Hong Kong*, 2002, pp. 304-311.

[8] C. Y. Dong and D. Y. Zhang, "On the side shapes of Women's breasts based on bra cups," *J. Zhejiang Fash. Inst. Technol.*, vol. 12, no. 3, pp. 23-27, 2013.

[9] F. Y. Wang, Y. Luo, and J. P. Wang, "Research on subdividing of female breast shape in Shanghai area," *Prog. Text. Sci. Technol.*, no. 4, pp. 73-76, 2012.

[10] Y. Kim and S. Lee, "A clustering validity assessment index," *Advances in Knowledge Discovery and Data Mining, Pacific-Asia Conference, Seoul, Korea, April 30 - May 2, 2003*.

[11] M. Halkidi, Y. Batistakis, and M. Vazirgiannis, "Cluster validity methods: part I," *Acm Sigmod Rec.*, vol. 31, no. 2, pp. 40-45, 2002.

[12] F. P. Kuhl and C. R. Giardina, "Elliptical fourier features of a closed contour," *Computer Graphics and Image Processing*, vol. 18, no. 3, pp. 236-258, 1982.

[13] Y. Liu, Z. Li, H. Xiong, and X. Gao, "Understanding of internal clustering validation measures," in *Proc. IEEE International Conference on Data Mining*, 2010, pp. 911-916.

[14] G. Chen, S. A. Jaradat, N. Banerjee, T. S. Tanaka, M. S. H. Ko, and M. Q. Zhang, "Evaluation and comparison of clustering algorithms in analyzing ES cell gene expression data," *Stat. Sin.*, vol. 12, no. 1, pp. 241-262, 2002.

[15] D. Arthur and S. Vassilvitskii, "k-means++: The advantages of careful seeding," in *Proc. the 18th Annual ACM-SIAM Symposium on Discrete Algorithms*, pp. 1027-1035, 2007.

[16] R. Tibshirani, G. Walther, and T. Hastie, "Estimating the number of clusters in a data set via the gap statistic," *J. R. Stat. Soc.*, vol. 63, no. 2, pp. 411-423, 2001.

[17] W. Gad, "SVM-Kmeans: Support vector machine based on Kmeans clustering for breast cancer diagnosis," *Int. J. Comput. Inf. Technol.*, vol. 5, no. 2, pp. 252-257, Mar. 2016.

[18] M. Halkidi and M. Vazirgiannis, "Clustering validity assessment: finding the optimal partitioning ofa data set," in *Proc. IEEE International Conference on Data Mining*, 2001, pp. 187-194.

[19] Y. Zhong, D. Li, G. Wu, and P. Hu, "Automatic body measurement based on slicing loops," *Int. J. Cloth. Sci. Technol.*, pp. 380-397, Apr. 2018.

[20] P. Hu, Y. Zhong, G. Wu, and D. Li, "Two-step registration in 3D human body scanning based on multiple RGB-D sensors," *J. Fiber Bioeng. Inform.*, vol. 8, no. 4, pp. 705-712, 2015.

Haoyang Xie received his master's degree in information assurance from the Fort Hays State University, KS, US, in 2011. He is currently pursuing a Ph.D. degree at Donghua University, Shanghai, China. His current research interests include 3D scanning technology, digital geometry processing, machine learning, and deep learning in 3D.

Xi Chen is now a lecturer at SIAS University, Xinzheng, China. She received the bachelor's degree in economics from Hubei University of Economics in 2008 and the master's degree from West Texas A&M University in 2012. Her current research interests include data mining, data analysis, and machine learning.

Zhicai Yu received the master's degree in textile material and textile design from Zhongyuan University of Technology, Zhengzhou, China, in 2015. He is currently pursuing a Ph.D. degree at Donghua University, Shanghai, China. His major is digital textile engineering. His work related to 3D scanning technology, image processing, machine learning, deep learning, fabric inquiry and analysis.

Yueqi Zhong is now a professor in the College of Textiles, Donghua University. He received the master's degree in textiles engineering from Xi'an Polytechnic University in 1982 and the Ph.D. degree in textile production design from Donghua University in 2001. He was a postdoctoral fellow Ph.D. the University of Texas at Austin from 2001 to 2005. His research interests include virtual garments, physically-based cloth simulation, geometry processing, interactive techniques, and deep learning.

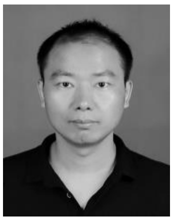

Kai Lu is now a lecturer in the College of Information Engineering, Xuchang University. He received the master's degree in computer application technology from Henan University of Science and Technology in 2009 and the Ph.D. degree in digital textile engineering from Donghua University in 2018. His research interests include textile image technology, computer vision and intelligent information processing.